



Aperture Measurements and Flow Experiments on a Single Natural Fracture

EVA HAKAMI†
ERIK LARSSON‡

The aim of the experimental work presented in the paper has been to carry out flow experiments and aperture measurements on the same specimen of a single natural fracture, in order to compare measured flow with predicted flow based on geometrical description of the fracture void space. A technique to measure the aperture was developed utilizing injection of fluorescent epoxy in the fracture specimen. An image analysis system was used to take measurements along sections across the fracture surface. The method was successfully applied to a fracture in granite having a mean aperture of 360 μm at 0.45 MPa normal stress. The spatial correlation of the aperture was about 1 cm. The predicted and measured flow through the fracture specimen are in good agreement. Copyright © 1996 Published by Elsevier Science Ltd.

1. INTRODUCTION

Recent concern about geological isolation of hazardous waste has created much interest in the field of ground water flow and solute transport. In crystalline rocks, flow occurs mainly in the fracture network. The flow properties of the fracture network are in turn governed by the flow properties of the single fractures. Therefore, one of the research needs is to be able to predict flow and transport in single fractures. The flow chart in Fig. 1 serves as a brief introduction to the problem of flow in single fractures, and illustrates the context of the experimental work that has been performed in this study.

If fluid flow is to be predicted, the factors that should be known are: the fluid property, the fracture void geometry and the fluid pressure at the boundaries. This work mainly concerns the fracture void geometry and how geometrical parameters can be defined and determined through aperture measurements.

Previous experimental work on flow in single fractures has mainly been concerned either with factors related to the geological history, explaining why there are differences in void geometry between fractures, or with the physical changes that may modify the void geometry (Fig. 1). The fracture conductivity as a function of normal stress has been studied by e.g. Witherspoon *et al.* [1], Barton *et al.* [2], Raven and Gale [3], Pyrak-Nolte

et al. [4], Sour and Hubbes [5] and Sundaram *et al.* [6]. The coupling between fracture conductivity and shear movement was investigated by Bandis *et al.* [7] and Makurat [8]. The differences in conductivity of fractures due to different geological histories have also been addressed [9,10]. On a large scale, field mapping of extension veins [11] and faults [12] have been used to study the relation between fracture length and aperture.

In situ investigations often include hydraulic tests in boreholes, where the flow response due to pressure changes is studied, see for example Doe and Osnes [13], Novakowski [14,15] and Rutqvist [16]. In both field and laboratory studies the parameter hydraulic aperture is commonly used. The hydraulic aperture is determined from the results of flow tests assuming that the fracture consists of two parallel plates. The hydraulic aperture is thus an equivalent aperture parameter.

To study the transport properties of fractures tracer experiments have been performed in the laboratory by Neretnieks *et al.* [17], Moreno *et al.* [18] and Haldeman *et al.* [19]. Tracer experiments have also been carried out on a field scale by Abelin *et al.* [20], Raven *et al.* [21] and Vandergraaf *et al.* [22]. Equivalent aperture parameters can be defined from the tracer experiments using travel time and the flow rate or travel time and hydraulic head [23].

Laboratory experiments aimed at obtaining a description of the fracture void geometry have been carried out by Gale *et al.* [24,25], Pyrak-Nolte *et al.* [4], Gentier *et al.* [26], Gentier [27], Hakami [28-30] and Iwano and Einstein [31]. They used different approaches to make the measurements: surface topography measurements,

†Division of Engineering Geology, Department of Civil and Environmental Engineering, Royal Institute of Technology, 10044 Stockholm, Sweden.

‡Department of Geology, Chalmers University of Technology, Gothenburg, Sweden.

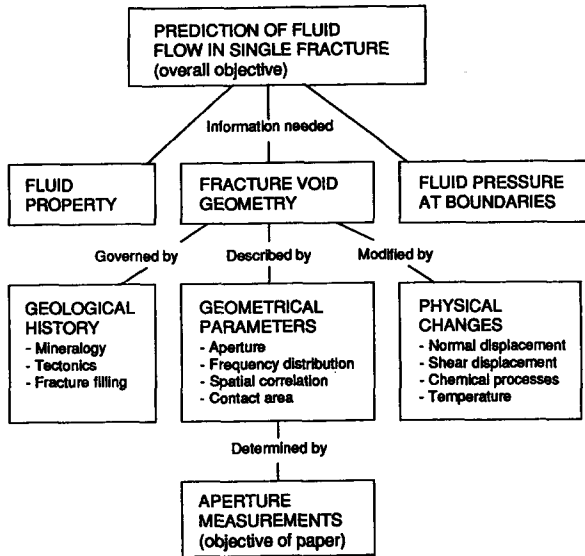


Fig. 1. Flow chart of experimental context.

casting or injection techniques [32]. However, the existing results on fracture void geometry are still very limited.

The aim of the experimental work presented in the following has been to develop techniques to carry out both flow experiments and aperture measurements on the same specimen of a natural fracture. The measured flow can thus be compared to the predicted flow based on geometrical parameters describing the actual void space.

2. DEFINITION OF APERTURE

The fracture void geometry is a complex three-dimensional structure. Geometrical parameters are to be established so that a useful characterization can be made of this kind of structure, see Hakami [33]. These parameters should make it possible to quantitatively describe the void space of a fracture and compare different individual fractures.

The term aperture is here defined as illustrated in Fig. 2. It is assumed that the fracture is parallel to an x - y -plane and that the aperture at each point is the separation distance between the fracture surfaces in the

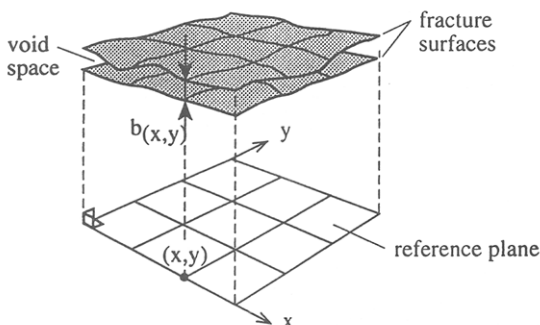


Fig. 2. Definition of aperture.

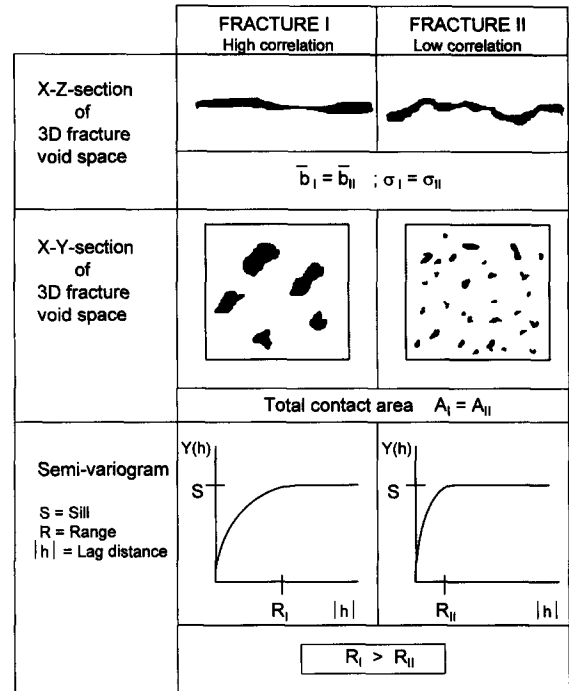


Fig. 3. Influence of spatial correlation on aperture distribution.

z -direction. the aperture is thus a pointwise distribution of values ranging from zero to a maximum value. Note that because of the roughness, the aperture is not the shortest distance between the two fracture surfaces at each point. The contact area is here defined as the areas where the apertures are smaller than a certain threshold.

A frequency distribution of apertures gives the probability that points with a certain aperture occur on the fracture surface. Experimental frequency histograms can, if desired, be approximated with different mathematical probability functions such as the normal, log-normal, Poisson or gamma distributions.

However, simply knowing the aperture frequency distribution is not enough to describe the entire pattern of the void geometry. Fractures with similar aperture frequency distributions may have different spatial correlation between the apertures on the fracture surface. Figure 3 illustrates how the spatial correlation influences the aperture pattern. Spatial correlation can be quantitatively studied with different geostatistical methods [34]. In this study (semi-)variograms have been used. A variogram shows the variation between pairs of data as a function of the distance between them (lag distance). The general difference in shape of variograms from fractures with different correlation is also indicated in Fig. 3. The plateau level of a variogram is called *sill* and the lag distance at which the sill is reached is called *range*.

There may be a need to describe the calculated "experimental" variograms (based on measured data) by idealizing the curve shape to a variogram model (cf. Fig. 3.) [34]. Variogram model functions (or covariance model functions) are needed when spatially correlated

stochastic variables are to be generated. Generated variable aperture fields have been used in numerical simulations of flow and transport in fractures by, for example, Moreno *et al.* [35].

3. EXPERIMENTAL WORK

3.1. Fracture description

The rock specimen containing the tested fracture is a medium-grained granite taken from the access tunnel of the Äspö Hard Rock Laboratory in south-eastern Sweden. The specimen was core drilled and contained a natural fracture lying almost parallel to the core axis. This fracture was intersected by a tight fracture, also subparallel to the core axis. The fracture specimen was kept undamaged during the sampling and was not opened at any time during the experimental work. The diameter of the core was 190 mm and it was 410 mm long.

3.2. Flow experiments

The equipment for the flow experiments was designed for drill core specimens containing fractures parallel to the core axis. The specimen was kept under compressive load by a biaxial cell during the experiments. Gauges were mounted on each end of the specimen to measure the deformation of the fracture during testing. A constant water head was supplied to the lower end of the specimen and the flow was measured from the overflow at the top [36]. The flow through the fracture was recorded for different confining pressures and water heads.

3.3. Aperture measurements

Figure 4 illustrates the different steps taken for aperture measurements. After the water flow experiments were completed the fracture was filled with a fluorescent epoxy resin. The sample was kept under confining stress in the biaxial cell during the injection and hardening of the epoxy. The core was cut into segments, using a diamond disc cutter, and each part was moulded in concrete. Each part was then cut along profiles across the fracture. After each cut, the aperture measurements were made along the exposed fracture profile using a stereo-microscope directly connected to an image analysis system [37]. With the aid of microscope filters, it was possible to obtain good contrast between rock and fluorescent epoxy. The image analysis system was programmed to measure the aperture at points with a specified distance along the profile. The accuracy of the measurements was about 10–30 μm with the image size used. At points where the fracture had two epoxy layers an equivalent aperture was calculated as $b = [b_1^3 + b_2^3]^{1/3}$.

The fracture studied most often has the features shown in Fig. 5(a) and (b). The surfaces are rather rough and the opposite surface profiles follow each other, thereby resulting in a fairly constant aperture. The photograph in Fig. 5(c) shows a point where the slopes of the fracture surfaces are steep. At these points the local perpendicular distance between the surfaces is smaller than the aperture as defined in this study. This illustrates the influence of the aperture definition on the measurement data (Fig. 2).

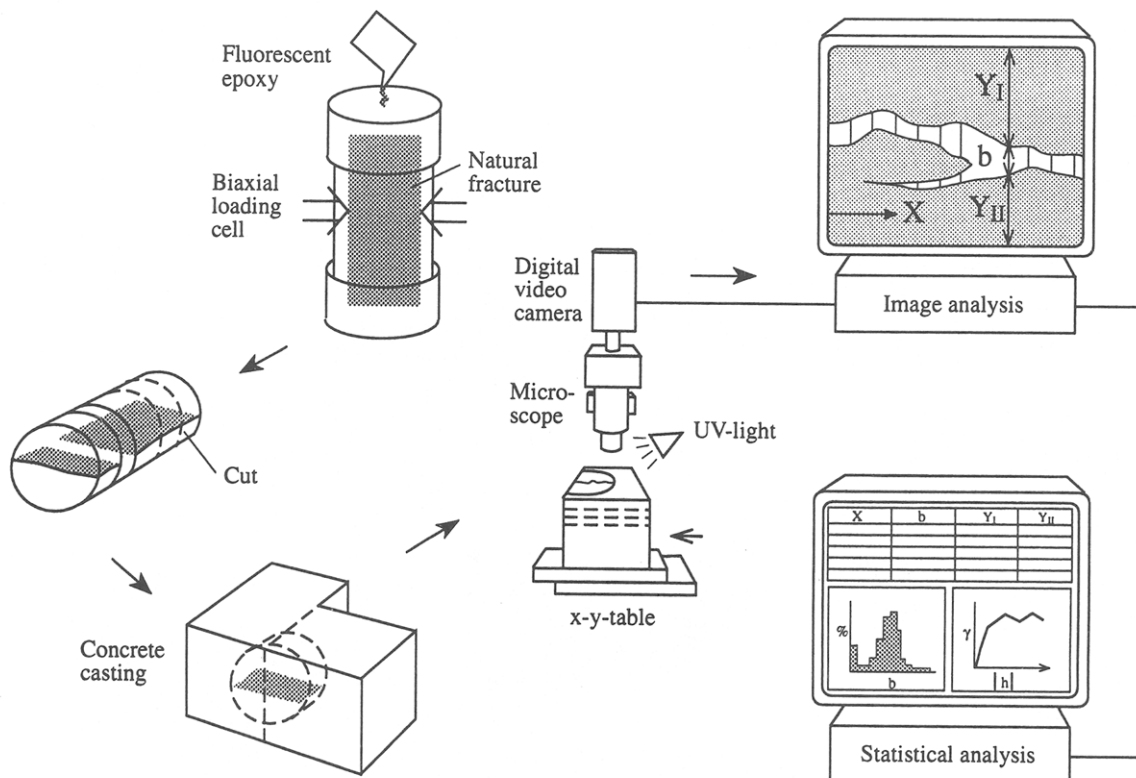


Fig. 4. Aperture measurement technique.

The fracture studied is intersected by another fracture, which has a very small aperture and did not contribute to the flow through the sample. Along the intersection of the two fractures, the fracture plane studied is displaced and the aperture is clearly affected [Fig. 5(d)].

At points where the fracture itself branches into several minor parallel fractures there will be a small-angle intersection. At these points the apertures are also affected with abrupt changes in the aperture as shown in Fig. 5(e) and (f). In this picture one can notice the fracture infilling of calcite. Other observed features are loose fragments inside the fracture [Fig. 5(g)] and air bubbles trapped in the epoxy [Fig. 5(h)]. At all points where the automatic measurements would become erroneous due to, e.g. air bubbles, fracture infilling of calcite or a damaged epoxy layer, the data were manually removed or corrected manually.

The surface profiles have at some points a very similar shape on both opposite sides. At these points the relative movements of the surfaces can be inferred. Figure 5(i) and (j) shows profiles in the direction parallel to the core axis, and Fig. 5(k) and (l) shows profiles in the direction perpendicular to the core axis. It can be noted that the displacement is small in both directions.

4. RESULTS

The flow rate measured for different water gradient and normal stress is shown in Fig. 6. The linear dependency between flow and water pressure gradient indicates laminar flow, as expected. Using the measured flow and water pressures, the hydraulic aperture was

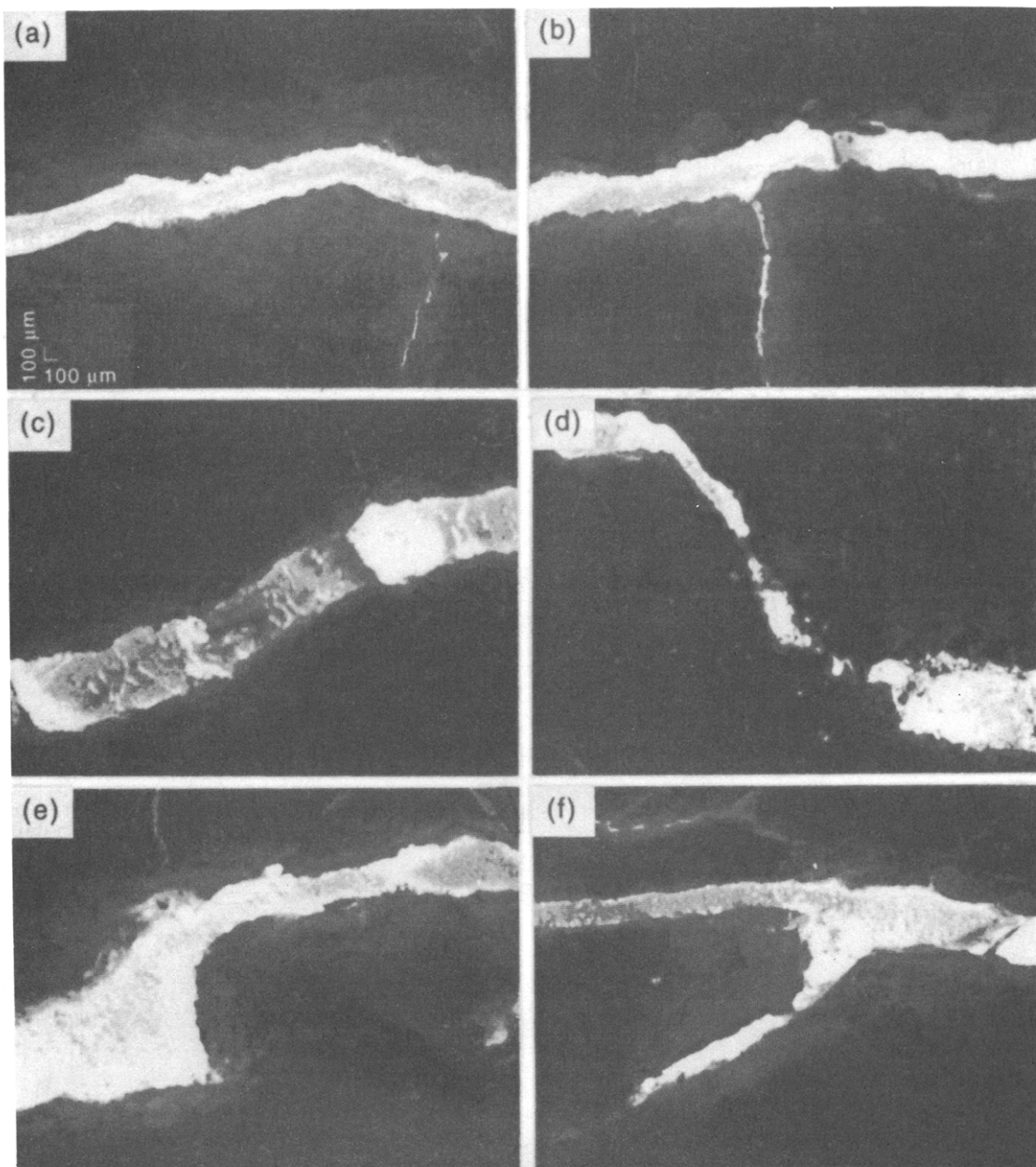


Figure caption opposite

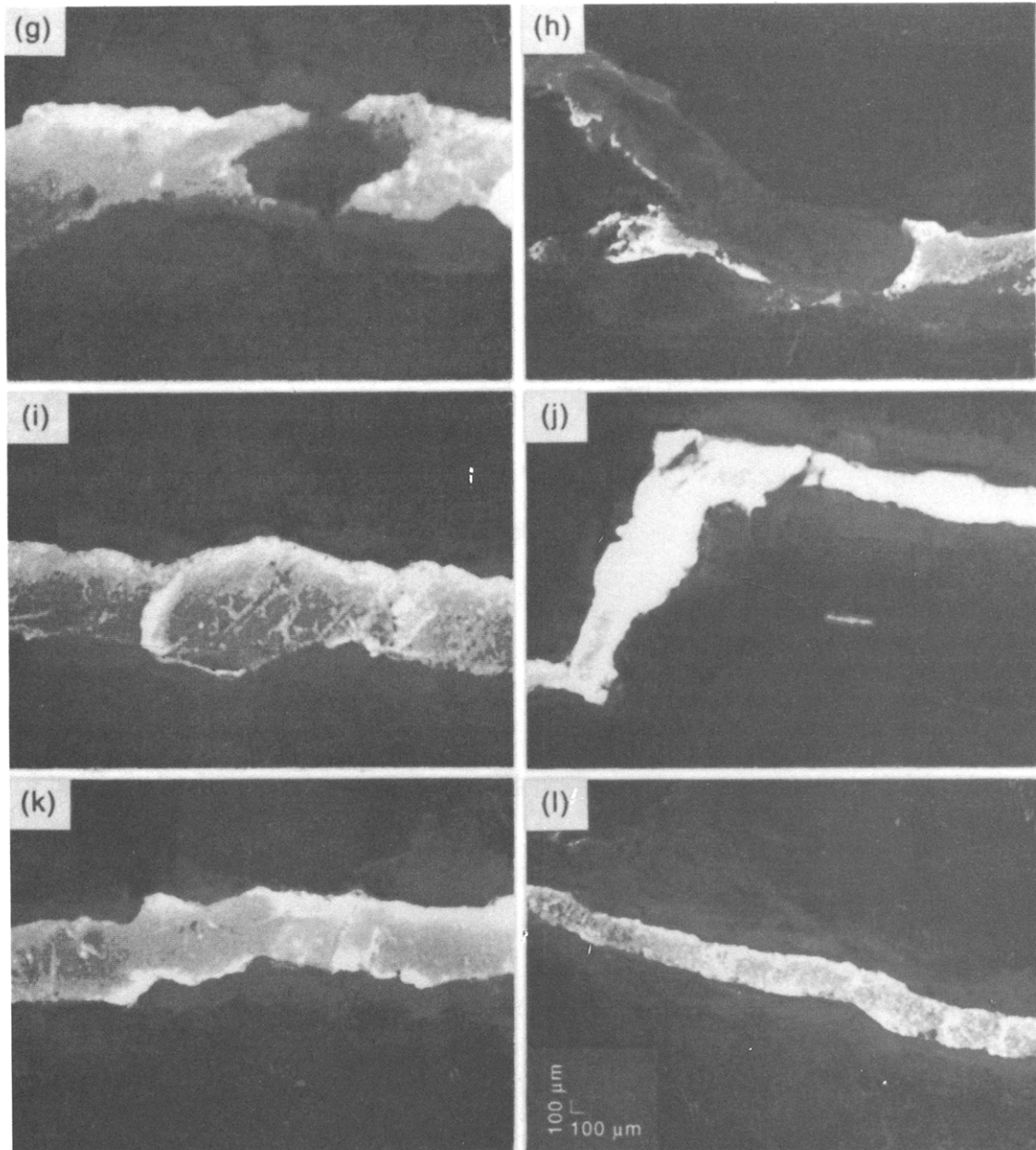


Fig. 5. Compilation of pictures from the aperture measurement: (a), (b) common shape of the fracture section; (c) locally inclined fracture surfaces (double scale); (d) intersection point between two fractures; (e), (f) branching point; (g) rock fragment (double scale); (h) air bubble trapped in the epoxy; (i) indication of fracture shear displacement (subarea B) (double scale); (j) indication of fracture shear displacement (subarea F); (k) indication of fracture shear displacement (subarea D) (double scale); (l) indication of fracture shear displacement (subarea E).

determined by the well known "cubic law". The hydraulic aperture at 0.45 MPa confining pressure was 250 μm (this low stress was selected since higher stress gave insufficient water flow to be accurately measured).

The deformation gauges on the inflow and outflow side of the specimen showed almost the same normal deformation. The normal stiffness of the fracture was about 24 GPa/m at 0.3–1.2 MPa. The difference in effective stress between the inflow and outflow sides of the specimen was about 20 kPa, and the water pressure head should thus only be responsible for a difference in average aperture, between the two sides, in the order of 1 μm .

RMMS 33/4—F

Figure 7(a) shows the configuration of the measurements taken on the studied fracture area. The size of the fracture is 190 \times 410 mm and the data are divided into eight subareas, A–H. The aperture was measured along profiles on the fracture surface, with a distance between data points of 200 μm for 65 profiles (100 μm for four profiles and 50 μm for one profile). A total of some 30,000 aperture data were recorded. The direction of profiles was changed between subareas in order to be able to pick up any possible anisotropy in the aperture pattern.

The spatial distribution of the aperture is understood by posting the location of data points with an aperture smaller than 50 μm [Fig. 7(b)]. It can be seen that these

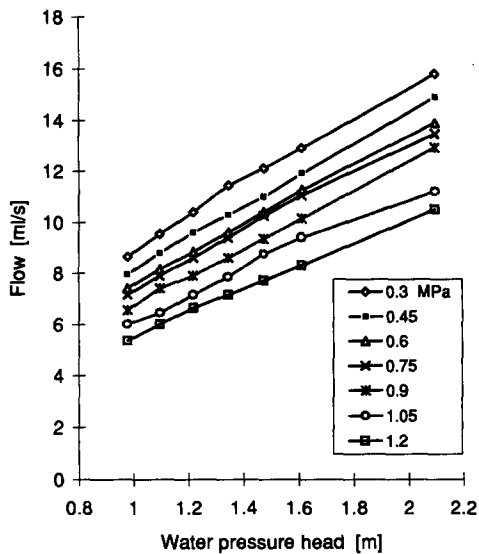


Fig. 6. Water flow vs gradient for different confining pressure.

“contact areas” are more frequent to the right of the specimen and correlated to the fracture intersection (dashed line) in particular in subarea B. The measurement profiles are oriented subparallel to the intersection in subareas D, E and G, and therefore the location and character of the intersection is not well known in the lower part of the specimen. The observation of slightly larger apertures on the left side of the specimen agrees with the results of the fluid transport test, where the first arrival appeared on the left-hand side [36].

Results of the aperture measurement of the eight subareas are presented as summary statistics in Table 1 and as frequency histograms in Fig. 8. The (arithmetic) mean of the subareas ranges from 307 to 380 μm , and the standard deviation lies between 133 and 321 μm . In general the shape of the frequency distributions is similar for all samples. The distributions are bell-shaped with a few percentage zero-apertures. Compared to a normal distribution they have a somewhat higher peak around the median. The mean aperture is slightly larger on the left-hand side of the fracture specimen. Also, the apertures are slightly larger at the inflow side compared to the out flow side of the specimen. Out of the total aperture data recorded, about 15% were taken at points with more than one epoxy layer.

In some of the images, the shear displacement of the two opposing surfaces could be estimated [cf. Fig. 5(i)–(l)]. Along profiles parallel with the core axis the displacement was 0–100 μm and along the profiles perpendicular to the core axis it was 150–250 μm .

The spatial correlation of the apertures has been analysed from variograms for each subarea using the computer code VARIOWIN [38] (Fig. 9). Apertures in the interval 0–1500 μm are included in the calculation of the variogram. For all samples, the range of the variograms is in the interval 5–20 mm. The range is largest in the subarea B where the contact area is also largest. The variograms for the fracture studied may be fairly

well approximated with an exponential model with a range ~ 8 mm and a sill $\sim 16,000 \mu\text{m}^2$.

Some of the variograms indicate a slight trend in the aperture, which causes the variogram to increase with lag distance without staying at a plateau. The same trend in the aperture, with slightly higher values to the left and to the inflow side of the specimen, can also be inferred from scatterplots of the apertures and from the summarized statistics as mentioned above. However, since this trend is small compared to the mean aperture of the fracture, it does not have a significant influence on the shape of the variograms or the interpreted correlation lengths.

Variograms were also calculated for data pairs in specified directions on the fracture surface. These “directional” variograms do not give any consistent result pointing at anisotropy in the spatial distribution of the fracture aperture. There is a tendency towards higher sill levels in the direction perpendicular to the core axis. This agrees with the observation of longer shear displacement in this direction.

The flow through the fracture has also been predicted using a variable aperture numerical model based on the measured aperture values [36]. The predicted flow was 27.7 ml/sec which should be compared to the experimentally measured 11.5 ml/sec (2.1 m water pressure head). The ratio between predicted and measured flow rate is thus 2.4.

5. DISCUSSION

The objective of the experiment was to develop techniques to measure the fracture void geometry of a natural fracture specimen which also was used in flow

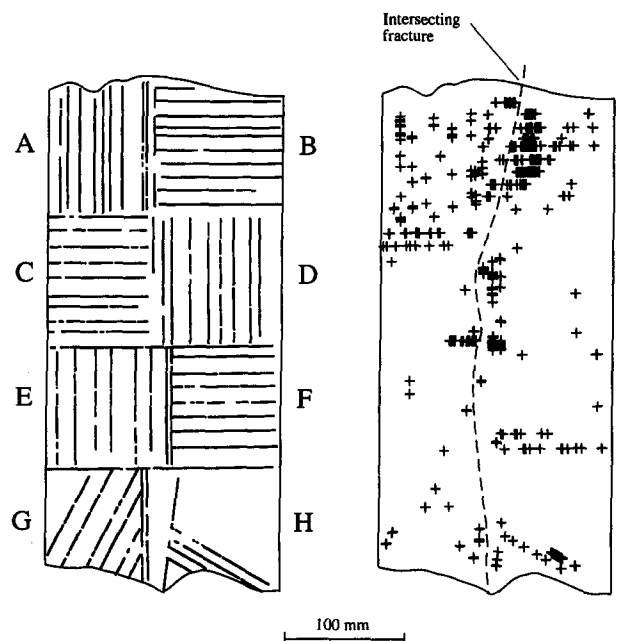


Fig. 7. (a) Configuration of measurement profiles and subareas; (b) location of measurement points with apertures smaller than 50 μm .

Table 1. Statistics of apertures in the subareas of the fracture

Subarea	A	B	C	D	E	F	G	H
Number of data points	5836	5825	3525	3840	3220	3468	2423	1679
Mean aperture, μm	365	307	380	349	384	358	379	360
Standard deviation	133	133	151	145	157	150	207	231
Median	366	317	373	338	358	331	336	321
$b < 50 \mu\text{m}$ (%)	5.5	7.0	3.0	3.5	0.5	0.7	0.7	3

tests, so that a direct comparison can be made between geometrical and hydraulic properties. This was made possible by a biaxial cell for the flow test, in combination with epoxy injection for the aperture measurements. One advantage of the methods employed is that they are very simple in principle and that the accuracy of the different measurements can be varied within a wide range. The accuracy of flow experiments can be enhanced, using more sophisticated devices for pressure, flow and deformation measurement. The aperture measurements can be made with different levels of accuracy, depending on the purpose of the study, by using different magnification of the pictures. To limit the measurement effort it may, in some cases, even be sufficient to cut a specimen only once and study the aperture along a single profile. The experimental set-up used also permits studies to be made of several intersecting and/or parallel fractures. It is also possible to adjust the water pressure device so that the flow is in the perpendicular direction, across the core axis.

The results presented are specific for the fracture studied and, as such, cannot be used for the prediction of flow in single fractures in general, but exemplify a natural aperture distribution. The measurement results from this study are summarized and discussed in the following.

The mean aperture of the fracture studied was about $360 \mu\text{m}$ at a confining stress of 0.45 MPa and the hydraulic aperture was about $250 \mu\text{m}$. The mean aperture of the fracture studied was thus 1.4 times larger than the hydraulic aperture. This is a ratio of the same order as those previously reported for fractures with a mean aperture 0.1 to 0.5 mm [2, 10, 27, 28, 39]. The lower value of the hydraulic aperture, compared to the "true" aperture, is expected since the variation in aperture of natural fractures forces the flow to be tortuous.

The "contact" area ($b < 50 \mu\text{m}$) for the fracture studied is small, less than 5%, which also agrees with earlier results for fractures under a low to moderate normal stress level ($< 1 \text{ MPa}$) [4, 40, 41].

In experiments with very high normal stresses across the fractures, the contact area may become considerably higher, up to 40% [4, 39–41]. In these cases, the mean aperture has been very small ($< 30 \mu\text{m}$). A very small contact area means that the surface area in contact with percolating water is large. This result may seem to contradict results from field experiments [5, 15, 20] indicating that flow occurs mainly in a few "channels". However, one of the explanations of this difference is that the aperture distributions of the fractures studied in

the field have had a different geological history with extensive shear displacements (minor faults and shear zones). Also, the apparent contradiction is explained by differences in the definition of parameters used. It should be noted that contact area is a purely geometrical property of the void space, and not a measure of the variation in flow velocities over the fracture surface area. A given aperture distribution will cause different flow patterns if the boundary conditions of the fracture are changed (cf. Fig. 1).

The uneven distribution of flow in rock fractures is often referred to with the term "channelling" (e.g. Ref. [17]). If by channelling we mean that the flow velocity varies between flow paths on a fracture surface, all fractures exhibit "channelling" to some extent, even if the contact area is small. Future research on the fracture void geometry will make possible quantitative studies of the "degree of channelling" and the flow distribution.

The result indicates that around 15% of the fracture area has a more complex geometry due to fragments or minor branching of the fracture. Although the fracture character was quite different, this result can be compared to the result from measurements on a highly conductive minor fault [30] where about 20% of the area showed this feature. This property of rock fractures may be important for the understanding of retardation processes in ground water transport of solutes.

From the result of spatial correlation, it can be concluded that the correlation length of the fracture aperture, 5–20 mm, is short compared to the size of the subareas (80 cm^2). This indicates that the sample size has been sufficiently large to capture the correlation of aperture on the specimen. However, possible *in situ* correlation, on a scale larger than the core sample, cannot be observed with the applied small-scale laboratory experiment.

It is also interesting to compare the correlation length of fracture apertures to the size of boreholes normally used for fracture investigations. If, as in this case, the correlation length is in the order of one centimetre or less, this is much smaller than the borehole diameter, and thus the results from borehole hydraulic tests on this type of fracture should not be very sensitive to borehole location.

The ratio between calculated flow, using a variable aperture model [35], and the flow measured in the experiment is 2.4. This result shows that the calculations slightly overestimate the measured fracture permeability. The difference in calculated and measured flow may be

partly ascribed to the approximation of the actual aperture distribution used in the numerical calculation [35]. No conductivity correction was made for the difference between the local perpendicular distance and the measured aperture (as defined in Fig. 2). Effects from branches and fragments were also ignored. The

errors in the aperture measurements may also have contributed to the discrepancy between measured and calculated fracture flow. Considering the factors just mentioned, the result of flow calculation is regarded as being in good agreement with the experimental result.

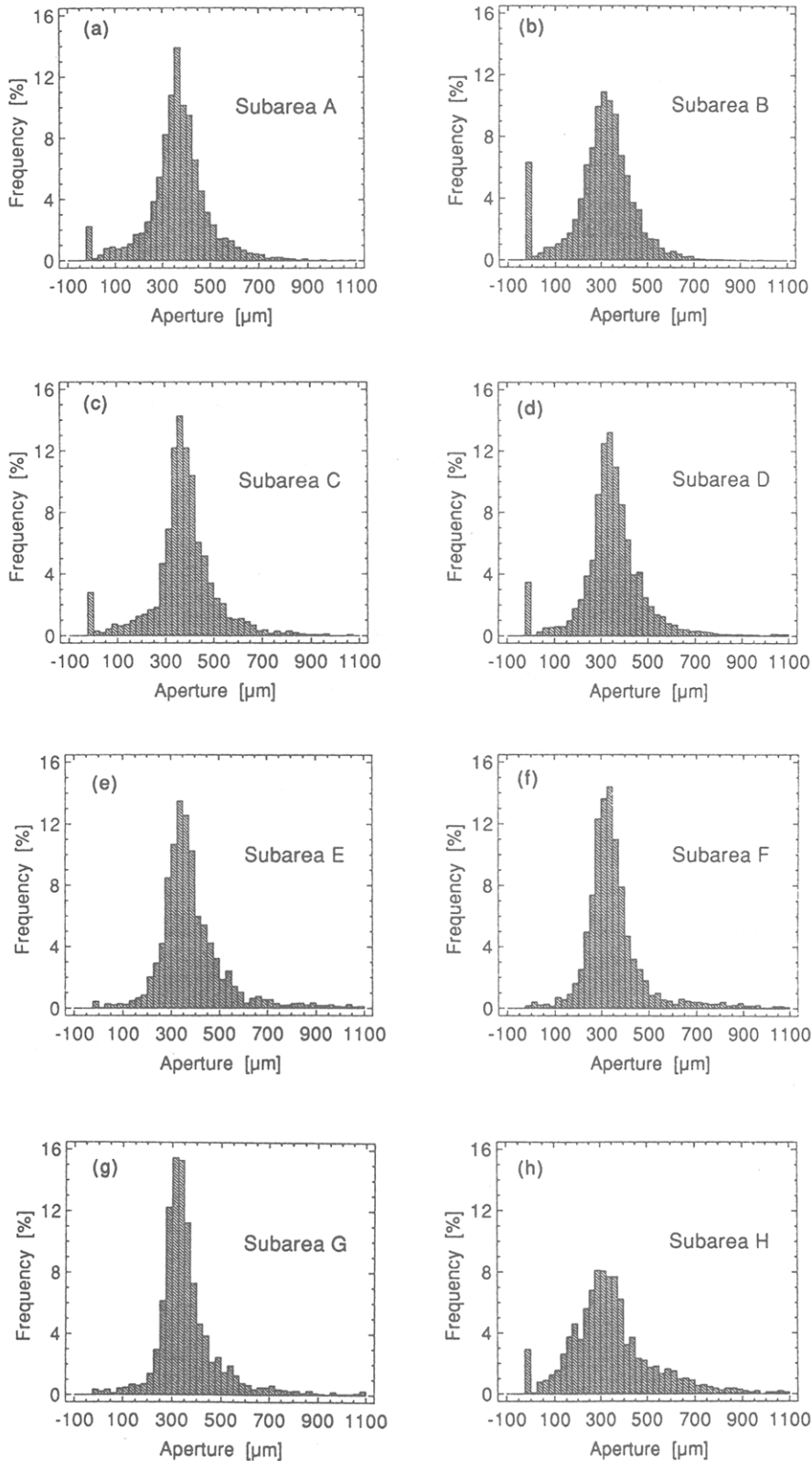


Fig. 8. Aperture distribution for the eight subareas of the studied fracture.

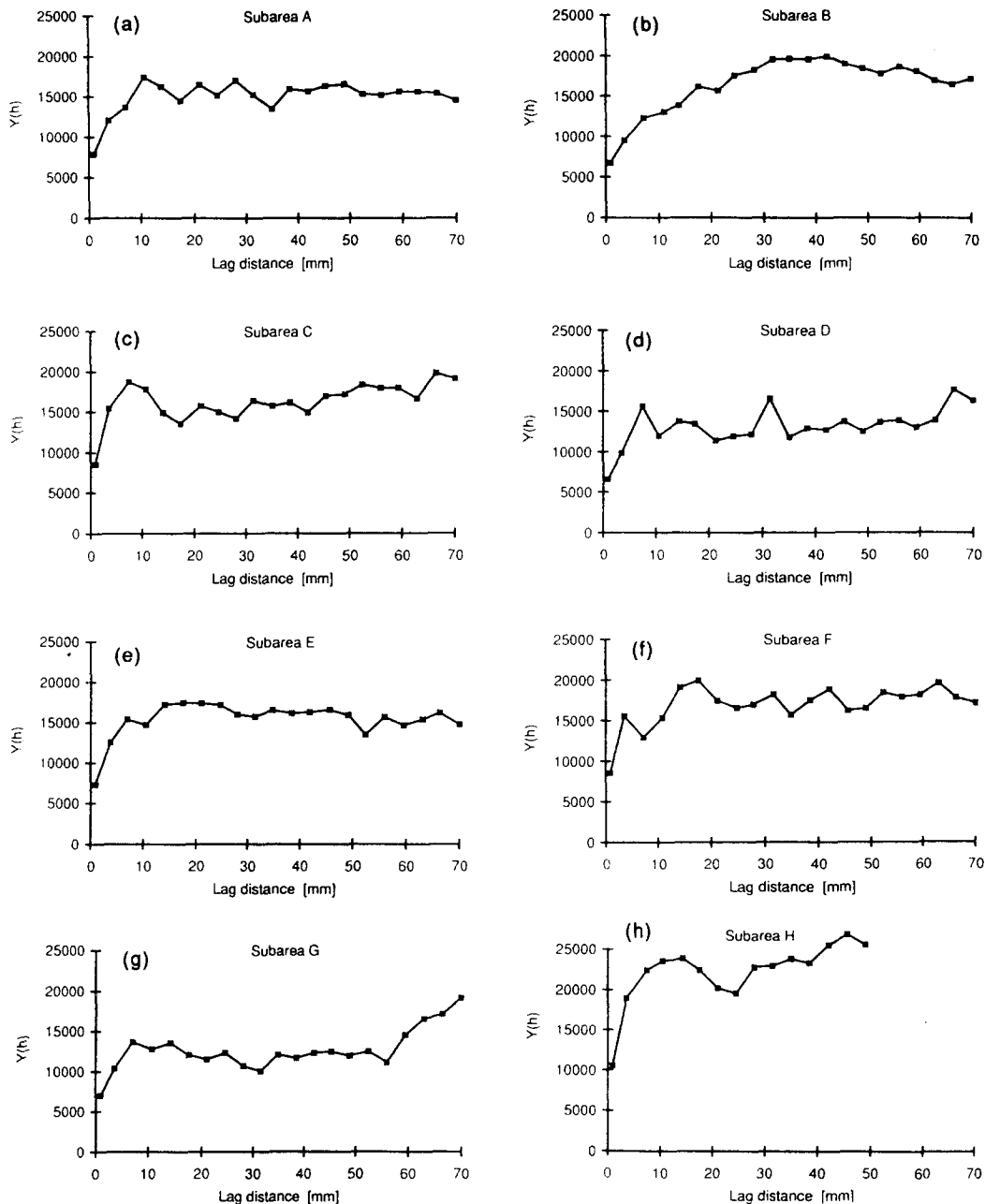


Fig. 9. Experimental variograms for the different subareas (omnidirectional).

6. CONCLUSIONS

The laboratory technique developed, utilizing epoxy injection and image analysis, has proved successful. The measurement method can provide data on the aperture distribution and aperture spatial correlation of a natural fracture specimen.

The method has been applied to a natural fracture specimen in granite. The mean aperture of this fracture is $360\ \mu\text{m}$ with a standard deviation of $150\ \mu\text{m}$, at a normal stress of $0.45\ \text{MPa}$ and the spatial correlation distance (range) is about one centimetre. Less than 5% of the fracture area has apertures smaller than $50\ \mu\text{m}$. The measured aperture data have been used to calculate the flow through the studied fracture. The ratio between calculated and measured flow is 2.4.

Acknowledgements—Financial support of this work provided by the Swedish Nuclear Fuel and Waste Management Co. (SKB) is gratefully acknowledged. We also thank Professor Ove Stephansson for his review of the manuscript.

Accepted for publication 2 August 1995.

REFERENCES

- Witherspoon P. A., Wang J. S. Y., Iwai K. and Gale J. E. Validity of cubic law for fluid flow in a deformable rock fracture. *Wat. Resour. Res.* **16**, 1016–1024 (1980).
- Barton N., Bandis S. and Bakhtar K. Strength, deformation and conductivity coupling of rock joints. *Int. J. Rock Mech. Min. Sci. & Geomech. Abstr.* **22**, 121–140 (1985).
- Raven K. G. and Gale J. E. Water flow in a natural rock fracture as a function of stress and sample size. *Int. J. Rock Mech. Min. Sci. & Geomech. Abstr.* **22**, 251–261 (1985).

4. Pyrak-Nolte L., Myer L. J., Cook N. G. W. and Witherspoon P. A. Hydraulic and mechanical properties of natural fractures in low permeability rock. *Proc. 6th ISRM Congr.*, Montreal, 1, 225–231 (1987).
5. Sour L. and Ubbes W. Fracture flow response to applied stress: a field study. *Proc. 28th U.S. Symp. Rock Mech.*, Tucson, Ariz. pp. 501–508 (1987).
6. Sundaram P. N., Watkins D. J. and Ralph W. E. Laboratory investigations of coupled stress-deformation—hydraulic flow in a natural rock fracture. *Proc. 28th U.S. Symp. Rock Mech.*, Tucson, Ariz. pp. 585–592 (1987).
7. Bandis S. C., Makurat A. and Vik G. Predicted and measured hydraulic conductivity of rock joints. *Proc. Fundamentals of Rock Joints*, Björkliden, Sweden, pp. 269–279 (1985).
8. Makurat A. The effect of sheer displacement on the permeability of natural rough joints. *Proc. Hydrogeology of Rocks of Low Permeability*, Tucson, Ariz. pp. 99–106 (1985).
9. Gale J. E. The effects of fracture type (induced vs natural) on the stress—fracture closure—fracture permeability relationship. *Proc. 23rd U.S. Rock Mech. Symp.*, Berkeley, Calif., pp. 290–296 (1982).
10. Iwano M. and Einstein H. H. Laboratory experiments on geometric and hydromechanical characteristics of three different fractures in granodiorite. *Proc. 8th ISRM Congr.*, Tokyo, pp. 743–750 (1995).
11. Vermilye J. M. and Scholz C. H. Relation between vein length and aperture. *J. Struct. Geol.* 17, 423–434 (1985).
12. Peacock D. C. P. and Sandersson D. J. Displacements, segment linkage and relay ramps in normal faults zones. *J. Struct. Geol.* 13, 721–733 (1991).
13. Doe T. and Osnes J. D. Interpretation of fracture geometry from well test. *Proc. Fundamentals of Rock Joints*, Björkliden, Sweden, pp. 281–292 (1985).
14. Novakowski K. S. Comparison of fracture aperture widths determined from hydraulic measurements and tracer experiments. *Proc. 4th Can./Am. Conf. Hydrol.*, Banff, Alberta, pp. 68–80 (1988).
15. Novakowski K. S. and Lapcevic P. A. Field measurement of radial solute transport in fractured rock. *Wat. Resour. Res.* 30, 37–44 (1994).
16. Rutqvist J. Coupled stress-flow properties of rock joints from hydraulic field testing. Doctoral thesis, Division of Engineering Geology, Royal Institute of Technology, Stockholm, ISBN 91-7170-829-4 (1995).
17. Neretnieks I., Eriksen T. and Tähtinen P. Tracer movement in a single fissure in granitic rock: some experimental results and their interpretation. *Wat. Resour. Res.* 18, 849–858 (1982).
18. Moreno L., Neretnieks I. and Eriksen T. Analysis of some laboratory tracer runs in natural fissures. *Wat. Resour. Res.* 21, 951–958 (1985).
19. Haldeman W. R., Chuang Y., Rasmussen T. C. and Evans D. D. Laboratory analysis of fluid flow and solute transport through a fracture embedded in porous tuff. *Wat. Resour. Res.* 27, 53–65 (1985).
20. Abelin H., Neretnieks I., Tunbrandt S. and Moreno L. Final report of the migration in a single fracture—experimental results and evaluation. Stripa Project, TR 85-03, SKB, Stockholm (1985).
21. Raven K. G., Novakowski K. S. and Lapcevic P. A. Interpretation of field tracer tests of a single fracture using a transient solute storage model. *Wat. Resour. Res.* 24, 2019–2032 (1988).
22. Vandergraaf T. T., Park C.-K. and Drew D. J. Migration of conservative and poorly sorbing tracers in granite fractures. *ANS*, Las Vegas, Nev. pp. 2251–2256 (1994).
23. Tsang Y. W. Usage of “equivalent apertures” for rock fractures as derived from hydraulic and tracer tests. *Wat. Resour. Res.* 28, 1451–1455 (1992).
24. Gale J., MacLeod R., Welham J., Cole C. and Vail L. Hydrogeological characterization of the Stripa site. Stripa Project, TR 87-15, SKB, Stockholm (1987).
25. Gale J., MacLeod R. and LeMessurier P. Site characterization and validation—measurement of flowrate, solute velocities and aperture variation in natural fractures as a function of normal and shear stress. Stripa Project, TR 90-11, SKB, Stockholm (1990).
26. Gentier S., Billaux D. and van Vliet L. Laboratory testing of the voids of a fracture. *Rock Mech. Rock Eng.* 22, 149–157 (1989).
27. Gentier S. Morphological analysis of a natural fracture. *Int. Assoc. Hydrogeol.*, pp. 315–326 (1990).
28. Hakami E. Water flow in single rock joints. Licentiate thesis 1988: 11L, Luleå Univ. of Technology, Sweden (1988).
29. Hakami E. and Stephansson O. Experimental technique for aperture studies of intersecting joints. *Proc. Eurock '93*, Lisbon, pp. 301–308, (1993).
30. Hakami E. Pore volume characterization—aperture distribution of a highly conductive single fracture. Åspölaboratoriet, Progress Report 25-94-30, SKB, Stockholm (1994).
31. Iwano M. and Einstein H. H. Stochastic analysis of surface roughness, aperture and flow in a single fracture. *Proc. Eurock '93*, Lisbon, pp. 135–141 (1993).
32. Hakami E., Einstein H. H., Iwano M. and Gentier S. Characterisation of fracture apertures—methods and parameters. *Proc. 8th ISRM Congr.*, Tokyo, pp. 751–754 (1995).
33. Hakami E. Aperture distribution of rock fractures. Doctoral thesis, Division of Engineering Geology, Royal Institute of Technology, Stockholm, ISBN 91-7170-835-9 (1995).
34. Isaacs E. H. and Srivastava R. M. *An Introduction to Applied Geostatistics*, p. 562. Oxford Univ. Press, New York (1990).
35. Moreno L., Tsang Y. W., Tsang C.-F., Hale F. V. and Neretnieks I. Flow and tracer transport in a single fracture: a stochastic model and its relation to some field observations. *Wat. Resour. Res.* 24, 2033–2048 (1988).
36. Larsson E. and Hakami E. Modelling of flow and transport in a single natural fracture. In preparation.
37. *IBAS2.5 User's Manual*, Kontron Elektronik GMBH (1994).
38. Pannatier Y. MS-Windows programs for exploratory variography and variogram modelling in 2-D. *Proc. Statistics of Spatial Processes: Theory and Applications*, Bari, Italy, pp. 167–170 (1993).
39. Gale J. E. Comparison of coupled fracture deformation and fluid flow models with direct measurements of fracture pore structure and stress-flow properties. *Proc. 28th U.S. Symp. Rock Mech.*, Tucson, Ariz. pp. 1213–1222 (1987).
40. Iwai K. Fundamental studies of fluid flow through a single fracture. Doctoral thesis, Univ. of California, Berkeley (1976).
41. Bandis S. C., Lumsden A. C. and Barton N. R. Fundamentals of rock joint deformation. *Int. J. Rock Mech. Min. Sci. & Geomech. Abstr.* 20, 249–268 (1983).